Surfactant Interactions and Solvent Phase Solubility Modulate Small Molecule Release from Emulsion Electrospun Fibers

Pamela M. Johnson[a], Justin M. Lehtinen[b], Jennifer L. Robinson*[a,b]

University of Kansas, [a]Bioengineering Graduate Program, [b]Department of Chemical and Petroleum Engineering

Manuscript Submitted to ***AICHE Journal***

Considered for Futures Issue

Abstract

Emulsion electrospinning represents a tunable system for the fabrication of porous scaffolds for controlled, localized drug delivery in tissue engineering applications. This study aimed to elucidate the role of model drug interactions with emulsion chemistry on loading and release rates from fibers with controlled fiber diameter and fiber volume fraction. Nile Red and Rhodamine B were used as model drugs and encapsulation efficiency and release rates were determined from poly(caprolactone) (PCL) electrospun fibers spun either with no surfactant (Span 80), surfactant, or water-in-oil emulsions. Drug loading efficiency and release rates were modulated by both surfactant and aqueous internal phase in the emulsions as a function of drug molecule hydrophobicity. Overall, these results demonstrate the role of intermolecular interactions and drug phase solubility on the release from emulsion electrospun fibers and highlight the need to independently control these parameters when designing fibers for use as tunable drug delivery systems.

Keywords: **Fibers, Emulsion Electrospinning, Controlled Drug Delivery/Release, Biomaterials, Biomedical Engineering**

Introduction

Electrospinning is a technique used in the fields of tissue engineering and drug delivery to develop tunable scaffolds with structural cues and the delivery of small molecules, peptides, and proteins to instruct tissue repair. The electrospinning platform has many advantages including the range of polymer and biologic systems that can be used to tailor release kinetics via diffusion, dissolution, and degradation mechanisms, high encapsulation efficiency, and high surface area-to-volume ratio for both cell interaction and drug release. Adaptations to the solution and setup including co-axial and emulsion electrospinning methods increase the ability to encapsulate phase-specific drugs and maintain the molecular structure and retention within the fibers. Emulsion electrospinning is particularly advantageous because of the additional ability to fine tune internal phase porosity and drug location, both of which are important factors for modulating release from the fibers, beyond what is achieved in traditional or co-axial electrospinning system. Controlling drug release from fibers is important to ensure that the drug is released at therapeutically effective concentrations while minimizing toxicity and adverse side effects to the patient. Numerous studies have been conducted to demonstrate that electrospun fibers are capable of encapsulating a wide variety of drugs, bioactive molecules, and proteins.[1-9] Fibrous mesh parameters including polymer degradation rate, fiber volume fraction and alignment, fiber diameter, and polymer-solvent drug compatibility have all been shown to control rate of drug release. However, the ability to independently control each of these parameters and understand the interaction of the drug and the electrospinning solution is difficult but must be of critical importance to understand for future designs of fibrous controlled release systems.

The fiber volume fraction and alignment of electrospun fibers play a critical role in drug release.[10] In a study by Xu et al., the fiber alignment and fiber volume fraction were shown to

affect overall fiber hydrophobicity and subsequent drug release.[10] Electrospun fiber volume fraction was increased through electrospinning fibers on a polymer film for increasing electrospinning times. Despite no changes in solution chemistry, as the time of electrospinning increased, the fiber volume fraction and corresponding contact angle also increased. Fiber volume fraction was only assessed qualitatively through the SEM images. These data indicate that at a higher fiber volume fraction, the overall mesh is more hydrophobic and contact with an aqueous liquid is less likely due to the trapping of air. Model drugs acetaminophen and 5-fluorouracil were released from a control polyvinyl butyral (PVB) film and from PVB electrospun fibers that were electrospun for time periods of 10, 20, and 60 minutes, respectively. Overall, the rate of drug release for both acetaminophen and 5-fluorouracil decreased with increasing fiber volume fraction. This indicates that fiber volume fraction may be playing a role in drug release rate, potentially due to solvent contact with fibers. Xu et al. also looked at the effect of fiber alignment on overall mesh hydrophobicity and the subsequent release of drugs from PVB electrospun fibers. Aligned electrospun fibers were compared to nonwoven, unaligned electrospun fibers. Aligned fibers had a lower contact angle compared to nonwoven, unaligned electrospun fibers. The higher contact angle observed in unaligned, nonwoven fibers may be due to pores creating more void space for air trapping. The subsequent release of model drugs acetaminophen and 5-fluorouracil both demonstrated a faster release rate from aligned fibers compared to nonwoven fibers. This further supports the hypothesis that as fiber volume fraction increases, mesh hydrophobicity also increases, creating less contact of the solvent with overall mesh and therefore reducing the rate of drug release.

The spacing and volume fraction of electrospun fibers, the diameter of the fibers, and the compatibility of the drug with the polymer-solvent system are all important in the rate of drug

release. In a study by Chen et al., the role of fiber diameter in drug release rate was shown.[11] Poly(lactic acid) fibers were loaded with 5-Fluorouracil as a model drug and electrospun with either a $CHCl_3$ and DMF solvent system or a 1,1,1,3,3,3-Hexafluoro-2-isopropanol (HFIP) and $CHCl_3$ solvent system. Processing parameters of flow rate and applied voltage were altered to achieve fibers with 1.02 µm ($CHCl_3$ and DMF), 0.73 µm ($CHCl_3$ and DMF), 0.53 µm (DMF and HFIP), and 0.35 µm ($CHCl_3$ and HFIP) diameters. Overall, fibers fabricated with both solvent systems demonstrated a larger burst release with larger fiber diameters. This was due to an increase in surface area of larger fibers allowing for more drugs to separate onto the surface of the fiber than in smaller fibers. Drug release after the initial burst demonstrated that the release rate from fibers with smaller fiber diameters was faster than in fibers with larger fiber diameters. This is because the diffusional path for a drug to diffuse from larger fiber diameters is longer than the diffusional path in smaller fiber diameters. Chen et al. also proposed that higher burst release may be due to drug solubility in the polymer-drug system but did not expand on this concept regarding their experimental results and chemistry of their solvents and drug. When analyzing the results of Chen et al.'s study, the model drug, 5-Fluorouracil, is a highly hydrophilic drug with a calculated partition coefficient of -0.9, according to PubChem. The dielectric constants, which are correlated to solvent polarity, of DMF, HFIP, and $CHCl_3$ are 36.7, 16.7, and 4.9, respectively.[12,13] Therefore, it would be expected that systems with less polar solvents are more likely to be incompatible with the highly hydrophilic model drug. In the study conducted by Chen et al., 5-Fluorouracil would be expected to have less compatibility in the systems fabricated with $CHCl_3$ and DMF solvents (F-3 and F-4) than in the systems fabricated with HFIP and DMF solvents (F-1 and F-2). This is indeed supported by the higher burst release of F-3 and F-4 compared to F-1 and F-2 fibers.

The importance of matching drug compatibility and polarity with the solvent and polymers used in electrospinning has been well documented.[4,14] Further, tuning of electrospun fibers can be achieved by using an emulsion. Emulsion electrospun fibers have the advantage of improved stability, bioavailability, encapsulation efficiency, and controlled release while also having the same control on fiber diameter, alignment, and fiber fraction as traditional solution electrospinning.[14] Increasing the concentration of surfactant in electrospun fibers can increase pores distributed throughout the fiber instead of coalesced within the core.[15] Samples with this distributed porous internal architecture are also known to have decreased burst and overall release rates.[15,16] Using an emulsion to fabricate fibers has also been shown to decrease drug release rate in systems with hydrophobic polymers.[15,17,18] Emulsion electrospinning is an attractive fabrication method to control drug release, improve encapsulation efficiency, and maintain bioavailability. Focusing on controlled release, it is important to understand the effects that surfactant, internal phase, and drug-polymer-solvent compatibility have on drug release from electrospun fibers. However, the effect of emulsion composition on small molecule release independent of the role of fiber diameter and fiber fraction has not been determined previously.

This study was designed to determine the role that drug hydrophobicity plays in fibers electrospun with no surfactant (control), surfactant, and water-in-oil emulsions in small molecule drug release when the effects of fiber diameter and fiber volume fraction have been controlled. Electrospinning solutions of all groups were fabricated with either Nile Red (hydrophobic) or Rhodamine B (hydrophilic) and short-term release was measured by releasing in sink conditions using an adequate solvent for each molecule. A least squares regression analysis for the best fit model was conducted to determine release mechanism and constant values. Overall, the findings from this work highlight the importance of emulsion composition on drug release, specifically the

impact of small molecule solvent phase preference and intermolecular interaction with the surfactant on release from the fibers, and will inform the design of more controlled release systems from emulsion electrospun fibers.

Materials and Methods

Materials

Poly(caprolactone) (PCL) (50,000 M_w) was purchased from CAPA lot # 120625. Span80 was purchased from Sigma Aldrich lot # MKCF4138. Solvent N, N-Dimethylformamide (DMF) anhydrous with 99.8% purity was purchased from Sigma Aldrich lot # SHBJ7641. Chloroform solvent ($CHCl_3$) with ≥ 99.5% purity was purchased from lot # SHBL1580. Anhydrous ethanol was purchased from Thermo Fisher Scientific lot # 201284. Nile Red with 99% purity was purchased from ACROS Organics lot # A0395995 and lot# 0082001. Rhodamine B with 99% purity was purchased from ACOS Organics lot # A0406070.

Electrospun Scaffold Fabrication

Polymer solutions were fabricated with PCL dissolved in 3:1 $CHCl_3$:DMF at a concentration of 20% w/v. Span80 was added to surfactant control with no internal phase and emulsion samples at a concentration of 30% w/v. Each solution was mixed for at least one hour on a stir plate with a stir bar spinning at a rate of 250 rpm, after which no solid polymer was visible in the solution. Model drugs, Nile Red or Rhodamine B, were then added to the solution at a concentration of 1 mg/mL, and the solution was mixed using a FlackTek Speed Mixer DAC 150.1FVZ-K for 30 seconds at a mixing speed of 2500 rpm. In samples containing the internal phase, water was added in 20 µL increments until a total of 8% w/o internal phase volume fraction was achieved. After each internal phase increment was added, the solution was mixed for 30 seconds at a mixing speed of 2500 rpm to ensure that internal phase droplets were adequately suspended within the continuous phase.

To compare the release of both a model hydrophilic and model hydrophobic drug from samples containing no surfactant, surfactant, and emulsion internal phase, the following samples were electrospun. Electrospinning parameters were held constant with a Harvard Apparatus pump flow rate of 1.5 mL/h, distance from needle tip to collection plate of 20 cm, an applied voltage of 18 kV from a GAMMA high voltage research source, and a blunted 21-gauge needle. All samples were loaded into a plastic 10 mL syringe for electrospinning. Samples using these processing parameters were electrospun for 20 minutes in a low relative humidity environment of 18% ± 3% and a temperature of 23 ± 2 °C. All samples were electrospun onto aluminum foil to avoid potential contamination of the collection plate with the model drugs Nile Red or Rhodamine B. After each sample was collected, it was carefully peeled off the collection plate and left to dry thoroughly in the fume hood overnight. Samples were further dried in a vacuum chamber before characterization. At least three samples were fabricated per set of sample parameters.

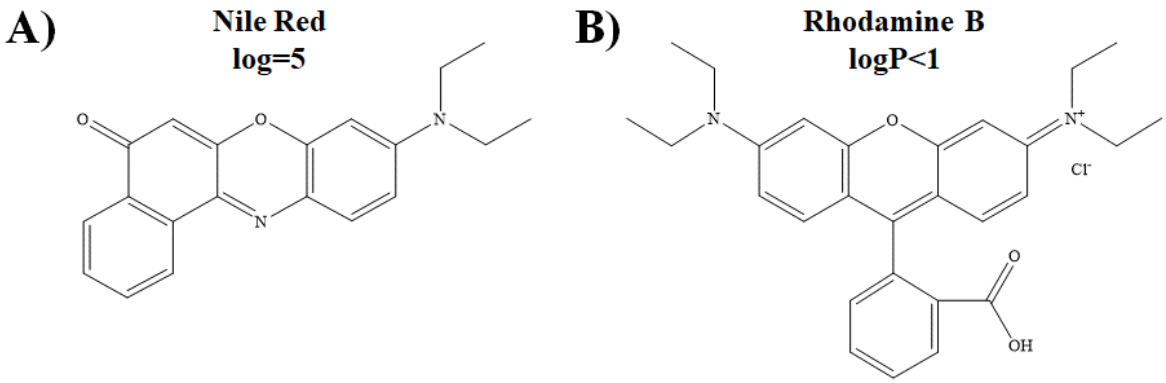

Figure 1: Chemical structures of model drugs Nile Red and Rhodamine B with their logP values.

To compare the effects of polymer-solvent compatibility with the hydrophobicity of a model drug, the model drugs Nile Red and Rhodamine B were encapsulated within fibers. Nile Red (logP = 5) is soluble in $CHCl_3$ and Rhodamine B (logP < 1) is soluble in water. [19,20] The structures of both small molecules are shown in Figure 1. Samples electrospun with these

parameters were fabricated using a solvent blend of 3:1 $CHCl_3$: DMF, have a model drug Nile Red (N) or Rhodamine B (R), have either no surfactant and no internal phase (N), surfactant and no internal phase (S), or surfactant and internal phase to make an emulsion (E). Therefore, samples with each of the following fabrication parameters will be known as NN, NS, NE, RN, RS, and RE, respectively, for brevity in Table 1 below.

Table 1: Sample Parameters for all electrospun mesh fabricated.

Acronyms							
First Position N= Nile Red R= Rhodamine B				Second Position N= No surfactant S= Surfactant E= Emulsion			
Sample Name	**Solvent**	**Surfactant Conc. (w/w %)**	**Internal Phase Volume Fraction (%)**	**Loaded Drug, Conc. (mg/mL)**	**Applied Voltage (kV), Pump Flow Rate (mL/h), Distance from Needle Tip to Collection Plate (cm)**	**Spinning Time (mins)**	**Range of Ambient Relative Humidity (%), Temperature (°C)**
NN (n=3)	3:1 $CHCl_3$: DMF	0	0	Nile Red, 1	18, 1.5, 20	20	16-17, 24.6-24.7
NS (n=3)	3:1 $CHCl_3$: DMF	30	0	Nile Red, 1	18, 1.5, 20	20	15-16, 24.5-24.6
NE (n=3)	3:1 $CHCl_3$: DMF	30	8	Nile Red, 1	18, 1.5, 20	20	15, 24.5-24.6
RN (n=3)	3:1 $CHCl_3$: DMF	0	0	Rhodamine B, 1	18, 1.5, 20	20	18, 24.3-24.5
RS (n=3)	3:1 $CHCl_3$: DMF	30	0	Rhodamine B, 1	18, 1.5, 20	20	21, 24.4-24.6
RE (n=3)	3:1 $CHCl_3$: DMF	30	8	Rhodamine B, 1	18, 1.5, 20	20	17-18, 24.4-22.5

Fiber Characterization

Mesh was analyzed using a Phenom Pro Desktop scanning electron microscope (SEM) to assess fiber morphology, surface topography, and diameter. Specimens were cut from the

electrospun samples in an approximately 1 cm x 1 cm square from the center of the collection to avoid potential edge effects. All samples were coated with 8 nm of iridium before imaging. Fiber morphology was characterized by imaging each sample in at least five different locations to capture morphological effects using 10 kV accelerating voltage, a backscatter detector, and a magnification appropriate to observe the fiber morphology. Fiber morphology was assessed for overall homogeneity and appearance of wet fibers. Fiber topography was determined through visual assessment and captured for samples electrospun at high relative humidity by imaging with 10 kV accelerating voltage, a backscatter detector, and at a magnification of 25,000x.

Fiber diameter was determined by imaging each sample specimen in five different locations using 10 kV of accelerating voltage and a backscatter detector. Locations were selected for each of the four corners of the square specimen and the central location. Mesh fabricated with $CHCl_3$ had larger fiber diameters and therefore was captured at a magnification of 1,000x. Mesh fabricated with 3:1 $CHCl_3$: DMF solvent had smaller fiber diameters and therefore was captured at a magnification of 5,000x. Each image was then analyzed with the software ImageJ using the plugin DiameterJ. From this initial segmentation, binary-colored segmented images produced with the algorithms M3, M5, M7, S2, S3, and S7 were used to determine fiber diameter and fiber diameter distribution using DiameterJ. In a few rare cases, DiameterJ was unable to process a segmented image, in which case a segmented image produced with an un-used algorithm that was judged as the most representative of the original image was substituted for further analysis. The average fiber diameter for each algorithm was then averaged to determine the average fiber per SEM image. These fiber diameters were then used for further statistical comparison between groups and plotted in GraphPad Prism.

The same binary-colored, segmented images from ImageJ used to determine fiber diameter were used to calculate the fiber fraction, which is described in Equation 5.1. Each image had all its white pixels, which represent the fiber area, and all the black pixels, which represent the void area, counted. The number of pixels representing fibers was divided by the total number of pixels and multiplied by 100 to calculate the percent fiber fraction.

$$Fiber\ Fraction = \frac{Fiber\ Area}{(Fiber\ Area + Void\ Area)} * 100 \quad (1)$$

Drug Loading

Specimens were cut from each electrospun mesh in triplicate using an 8 mm diameter histology punch. Each specimen was weighed to normalize for localized differences in mesh thickness. Each mesh was then dissolved in 2 mL of $CHCl_3$ and manually mixed by shaking until the mesh visually appeared to be entirely dissolved in the solvent. Each solution was then mixed using a vortex, and 200 µL of the solution was pipetted in triplicate into a black 96 well plate. Within the same well plate, standards of the drug in known concentrations were prepared with a serial dilution in $CHCl_3$. For RN, RS, RE, NN, NS, and NE samples, concentrations of standards were 50, 10, 2, 0.4, 0.08, and 0.016 µg/mL. To compensate for any potential interactions between the fluorescent drugs and the surfactants, additional standards that included surfactants were made at the same concentrations (Figure 3D and 5D). In the case of Rhodamine B, the effect of surfactant on the fluorescence was dramatic, significantly lowering the fluorescence at all concentrations. Meshes that included surfactant were analyzed against standards that included surfactant and meshes without surfactant were analyzed against standards without surfactant. All samples were measured for fluorescence using a Biotek Cytation 5 microplate reader. Samples loaded with Nile Red were measured using an excitation of 552 ± 20 nm and emission at 636 ± 20 nm, and samples

loaded with Rhodamine B were measured using an excitation of 553 ± 20 nm and emission at 627 ± 20 nm. Concentration was calculated for each mesh using the standard curve and normalized per weight of each individual mesh.

Drug Release

Specimens were cut from each electrospun mesh in triplicate using an 8 mm diameter histology punch. Each specimen was weighed to normalize for localized differences in mesh thickness. Each specimen loaded with either Nile Red or Rhodamine B was placed in 1 mL of ethanol or RO water, respectively. At time points of 0.5, 1, 1.5, 2, 2.5, 3, 4, 5, 10, 15, 30, 45, and 60 minutes, the solvent was removed and stored temporarily in an Eppendorf tube for future analysis of concentration and the solvent in the specimen tube was replenished. Stored samples were covered in aluminum foil to minimize the effects of photobleaching. Upon completion of the collection of each sample, aliquots were mixed before 200 µL aliquots were removed from the sample and pipetted into 96 well plates in triplicate. All samples loaded with Nile Red were measured for fluorescence using a Biotek Cytation 5 microplate reader with an excitation of 554 ± 20 nm and emission at 638 ± 20 nm. All samples loaded with Rhodamine B were measured for fluorescence using a Biotek Cytation 5 microplate reader with an excitation of 553 ± 20 nm and emission at 627 ± 20 nm. Concentration was determined with a standard curve of the drug in release media. Standard curves of Nile Red in ethanol were prepared using a serial dilution to create concentrations of 0.01, $2x10^{-3}$, $4x10^{-4}$, $8x10^{-5}$, and $1.6x10^{-5}$ mg/mL. Rhodamine B's standard curves in water were prepared with a serial dilution to create concentrations of 0.01, $2x10^{-3}$, $4x10^{-4}$, $8x10^{-5}$, and $1.6x10^{-5}$ mg/mL.

Best Fit Model using Regression Analysis

The experimental drug release data was compared to four established models: zero-order first-order, Higuchi[21], and Ritger-Peppas (non-swellable, cylinders)[22] release. The equations used for each model are shown below (Equations 2-5).

$$Zero-Order: \frac{M_n}{M_\infty} = Kt \tag{2}$$

$$First-Order: \frac{M_n}{M_\infty} = 1 - e^{(-Kt)} \tag{3}$$

$$Higuchi: \frac{M_n}{M_\infty} = Kt^{0.5} \tag{4}$$

$$Ritger-Peppas: \frac{M_n}{M_\infty} = Kt^n, n = 0.45\ (assuming\ Fickian\ diffusion) \tag{5}$$

Microsoft Excel with the solver add-in package was used determine the best fit K value for each model by calculating the K value that would minimize the square root sum of the residuals. Each model then had its fit checked against the data by calculating the R^2 value according to the following equation (Equation 6).

$$R^2 = 1 - \left(\frac{\sum(y_t - m_t)}{\sum(y_t - \bar{y})}\right) \tag{6}$$

Statistical Analysis

Fiber diameter per SEM image was determined with ImageJ and the plugin DiameterJ as described above. The average fiber diameter of each SEM image was used to compare fiber diameter and fiber fraction between groups. First, a one-way ANOVA with Brown-Forsythe and Welch's tests was performed on each set of sample parameters, respectively, to determine that the

electrospun samples were statistically different. This was followed up with Dunnett posthoc test. Groups were compared using a one-way Brown-Forsythe and Welch's ANOVA with Dunnett's multiple comparisons posthoc and 95%, 99%, 99.9%, and 99.999% confidence intervals.

The drug loading was compared using the average amount encapsulated in a specimen calculated using the average per well on the well plate's theoretical concentration based on the standard curve. The average concentration in each specimen was used to compare the set of sample parameters for respective groupings. The comparison was performed using Welch's test for pairwise comparisons and one-way ANOVA for Brown-Forsythe and Welch's tests and 95%, 99%, 99.9%, and 99.999% confidence intervals. Data with confidence intervals were plotted between respective groups on boxplots to show variance in the data. The amount of cumulative drug release was normalized by the individual samples' weight and plotted relative to the theoretical amount of drug encapsulated w/w%. All statistical tests and graphing were performed using Prism Graphpad software.

Results and Discussion

To determine the effects of surfactant and internal phase on the drug release, both a hydrophobic and hydrophilic small molecule model drug, Nile Red ($logP=5$)[20] and Rhodamine B ($logP<1$)[20], respectively, were loaded and electrospun into fibers. A solvent system of 3:1 $CHCl_3$: DMF at low relative humidity was used to ensure that the fibers had comparable fiber diameters and fiber fractions between all groups. This was important to ensure that observed differences were not because of fiber diameter, surface topography, or mesh volume fraction, all of which are known to affect drug release from electrospun fibers. Further, all fibers were electrospun at low relative humidity to minimize the effects of ambient water vapor that leads to vapor induced phase separation and surface roughness.

Fibers Loaded with Nile Red – Fiber Morphology, Diameter, and Fiber Fraction

Fibers encapsulated with Nile Red containing no surfactant (NN), surfactant (NS), and internal phase of 8% w/o to create an emulsion (NE) had average fiber diameters of 0.70 ± 0.48, 0.56 ± 0.33, 0.62 ± 0.26 µm, respectively (Figure 2A). The fiber morphology for these samples was predominantly uniform and cylindrical, with some smaller fibers. The distribution of fiber diameter decreased with the addition of the internal phase, and the surface topography of all these fibers was smooth. Uniform fiber topography is important because it influences air trapping and resulting media contact with the mesh and, therefore, drug release. Fiber topography was smooth

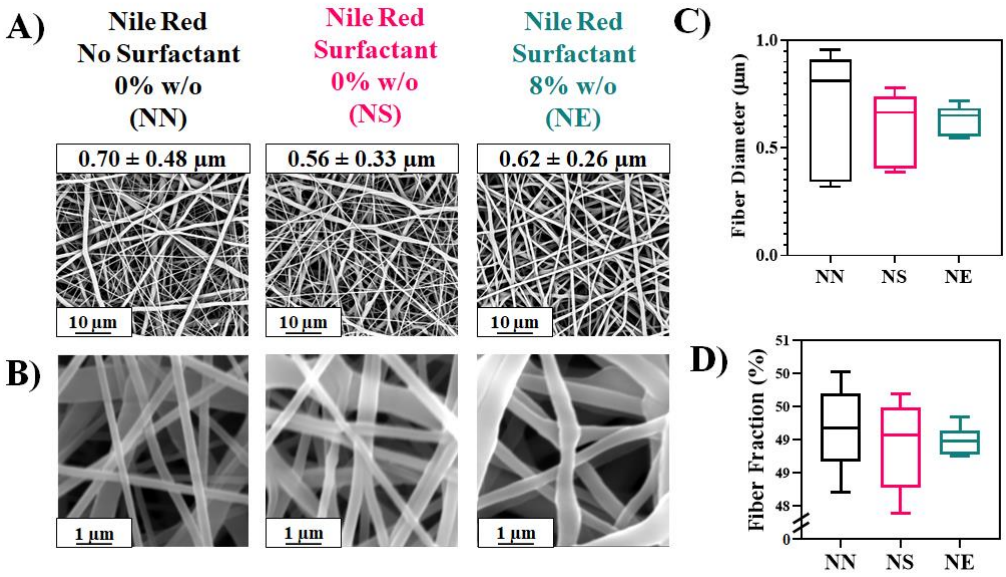

Figure 2: Fiber morphology, diameter, and fiber fraction for Nile Red encapsulation and release. A) Representative SEM images of electrospun fibers loaded with Nile Red without surfactant (NN), with surfactant (NS), and with both surfactant and internal phase volume fraction at 8% w/o to form an emulsion (NE). B) Representative SEM images of fiber surface topography. C) Average fiber diameter and standard deviation calculated for all fibers in the sample. D) Average fiber volume fraction percent for each SEM image plotted in a boxplot. * $p \leq 0.05$; ** $p \leq 0.01$; *** $p \leq 0.001$; ****$p \leq 0.0001$

because all fibers were electrospun at low relative humidity, so insufficient ambient water vapor was present to template porosity by a vapor induced phase separation (VIPS) mechanism (Figure 2B). Fiber diameters (Figure 2C) and fiber volume fraction (Figure 2D) were not statistically

different for NN, NS, and NE samples, indicating that fiber diameter and fiber volume fraction are relatively equivalent and differences in release observed in these groups is not due to fiber diameter or fiber volume fraction.

Fibers Loaded with Nile Red – Drug Loading and Release

Electrospun fibers collected from each group with Nile Red encapsulated are shown in Figure 3A. The amount of drug loaded in NN, NS, and NE was statistically different for each group (Figure 3B). The highest levels of loading were in NN samples, followed by NS samples and finally NE samples. Santhanalakshmi et al. found that due to intermolecular interactions between $CHCl_3$ and DMF, the aggregation of Tween 80 was higher in this blend of solvents than the pure

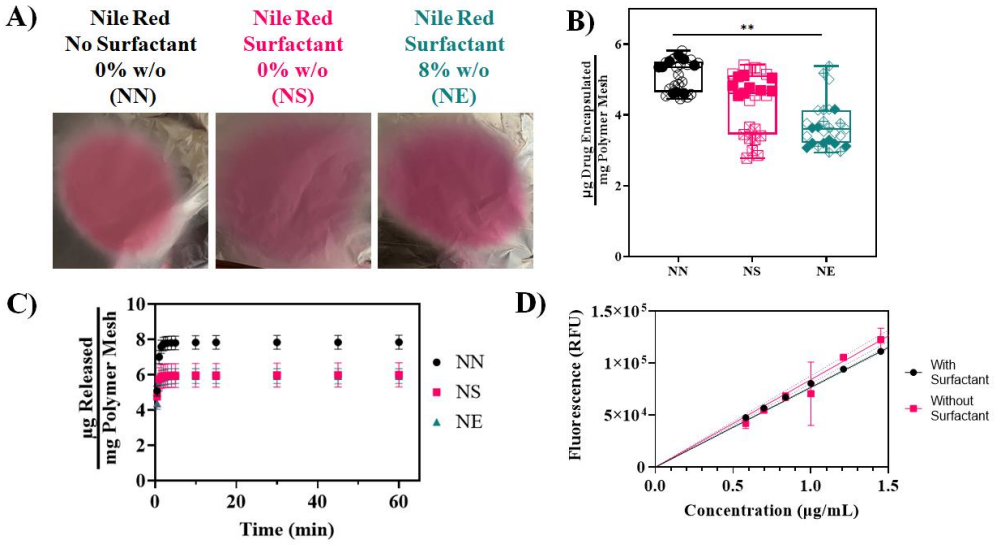

Figure 3: Nile Red encapsulation and release from fibers without surfactant (NN), with surfactant (NS), and with both surfactant and internal phase volume fraction at 8% w/o to form an emulsion (NE). A) Visual of collected fibers on plate with Nile Red encapsulated. B) Amount of Nile Red encapsulated in 8 mm electrospun mesh punch samples. C) Mass of Nile Red released over one hour for samples fabricated and normalized by weight of individual sample mesh. D) Standard curve illustrating minimal effect of interaction of the surfactant with the Nile Red on fluorescence values. * $p \leq 0.05$; ** $p \leq 0.01$; *** $p \leq 0.001$; ****$p \leq 0.0001$

solvents individually.[23] This could also be true for Span 80 and Nile Red in a blend of these solvents. Further, hydrogen bonding can also cause associations of Span 80 and Nile Red, resulting

in larger aggregated Span 80- Nile Red complexes to flocculate and a small degree of sedimentation during electrospinning. Small amounts of sedimentation would account for lower encapsulation of Nile Red in NS samples compared to NN samples, but overall differences in encapsulation are marginal. The emulsion samples (NE) had significantly lower amount of encapsulated Nile Red than the surfactant samples (NS). This result was not expected and may have been due to experimental error or a degree of phase separation when water was added to the system.

All groups with Nile Red experienced burst release and comparable release profiles (Figure 3C). The release rates of NS and NE were quite similar and highlight that Nile Red is not completely compatible with this polymer-solvent system even with the addition of surfactant. Nile Red in these systems is likely forced to the surface through a combination of electrostatic repulsion and phase separation. Nile Red is a small molecule with a preference for organic solvents. Therefore, in systems with a mixture of 3:1 $CHCl_3$: DMF, Nile Red will prefer the $CHCL_3$ to DMF. Figure 3D illustrates minimal effect of Nile Red interactions with Span 80 on fluorescence values using a standard curve with Nile Red.

Fibers Loaded with Rhodamine B- Fiber Morphology, Diameter, and Fiber Fraction

Fibers encapsulated with Rhodamine B containing no surfactant (RN), surfactant (RS), and emulsion with internal phase of 8% (RE) had average fiber diameters of 0.44 ± 0.21, 0.49 ± 0.26, and 0.58 ± 0.26 μm, respectively (4A). The fiber morphology for these samples was predominantly uniform and cylindrical, with some smaller fibers. The distribution of fiber diameter decreased with the addition of the internal phase. The surface topography of all these fibers was smooth (Figure 4B) because all fibers were electrospun at low relative humidity, so insufficient ambient water vapor was present to template surface porosity. Differences in fiber diameter between RN,

RS, and RE were not statistically different (Figure 4C). When fiber diameter is not statistically

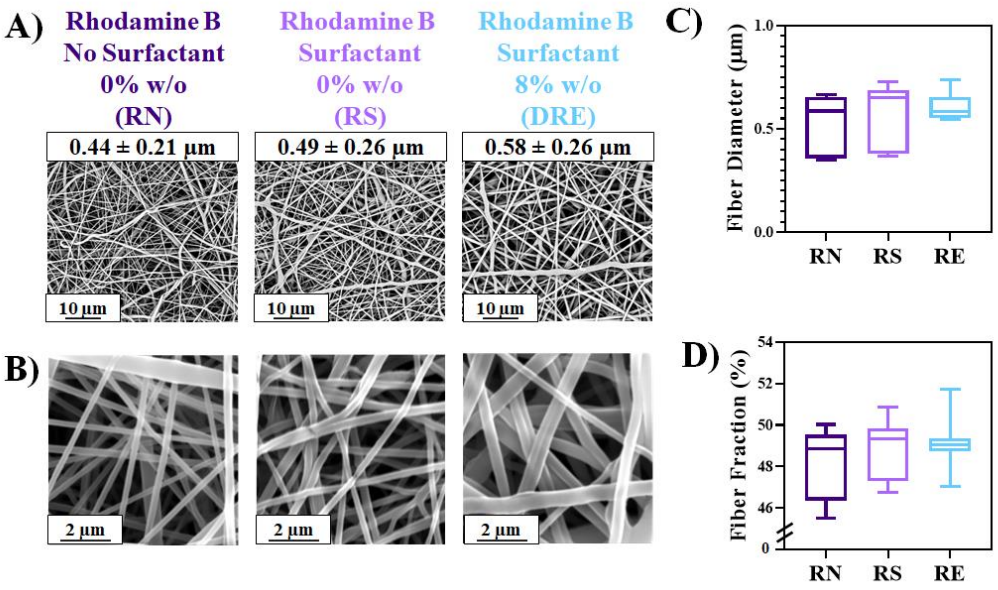

Figure 4: Fiber morphology, diameter, and fiber fraction for Rhodamine B encapsulation and release. A) Representative SEM images of electrospun fibers loaded with Rhodamine B without surfactant (RN), with surfactant (RS), and with both surfactant and internal phase volume fraction at 8% w/o to form an emulsion (RE). B) Representative SEM images of fiber surface topography. C) Average fiber diameter and standard deviation calculated for all fibers in the sample. D) Average fiber volume fraction percent for each SEM image plotted in a boxplot. * $p \leq 0.05$; ** $p \leq 0.01$; *** $p \leq 0.001$; ****$p \leq 0.0001$

different, it is unlikely to play a major role in drug release. Fiber volume fraction was not statistically different between DRM, RS, and RE samples, indicating that it also is unlikely to play a major role in drug release (Figure 4D). Standardizing fiber diameter and fiber volume fractions across samples is essential to thoroughly compare solution and drug solubility parameters.

Fibers Loaded with Rhodamine B - Drug Loading and Release

Visual changes in the color of collected mesh with Rhodamine B as a function of composition are seen in Figure 5A, illustrating interactions of the small molecule with the surfactant and water phase. The amount of Rhodamine B loaded in the emulsion fibers (RE) was significantly larger than the control (RN) and fibers with solely surfactant (RS) (Figure 5B). In the

RN and RS groups, the loading of Rhodamine B was lower compared to the emulsions (RE) because Rhodamine B has low solubility in $CHCl_3$, and therefore some phase separation would cause lower amounts of the drug to be encapsulated in the fibers. RE groups exhibited the highest loading because Rhodamine B predominantly prefers the water internal phase of the fibers. This result is significant because it proves that using an internal phase and a surfactant can improve the loading of hydrophilic molecules in hydrophobic solvent-polymer systems. This is consistent with other studies loading hydrophilic drugs within emulsions in the field.[14,24-26] Future work will

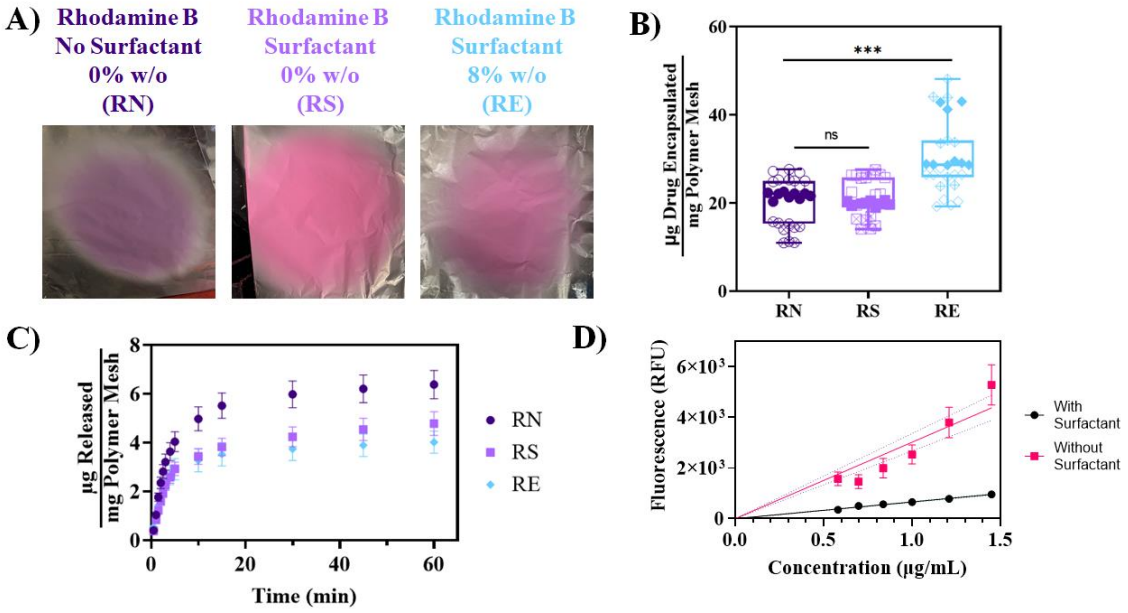

Figure 5: Rhodamine B encapsulation and release from fibers without surfactant (RN), with surfactant (RS), and with both surfactant and internal phase volume fraction at 8% w/o to form an emulsion (RE). A) Visual of collected fibers on plate with Rhodamine B encapsulated. B) Amount of Rhodamine B encapsulated in 8 mm electrospun mesh punch samples. C) Mass of Rhodamine B released over one hour for samples fabricated and normalized by weight of individual sample mesh. D) Standard curve illustrating the interaction of the surfactant with the Rhodamine B and impact on fluorescence values. * $p \leq 0.05$; ** $p \leq 0.01$; *** $p \leq 0.001$; ****$p \leq 0.0001$

investigate increasing hydrophilic drug loading by increased internal phase volume fraction.

The release of Rhodamine B from RN had the biggest burst release because Rhodamine B has poor solubility in $CHCl_3$, and charge repulsion forced it to the surface of the fiber (Figure 5C). The burst release for RS and RE were significantly lower than RN. In RE groups, Rhodamine B preferred the internal phase, and therefore most was protected from burst release. RS is slightly higher than RE in drug release rate after the burst, possibly because there is less internal phase, or the internal phase did not have as much time to coalesce once inside the fiber. This same reduction in burst release and reduction in overall release rate has been observed in several other electrospinning studies.[15,17,27,28] However, in all of these studies, the comparison of no surfactant, surfactant, and emulsion has not been made between fibers with insignificant differences in fiber diameter and fiber volume fraction, potentially leading to other confounding variables in release profiles. Interestingly, the burst release of Rhodamine B from fibers containing surfactant and emulsion fibers was quite similar. This indicates that surfactant alone may reduce the burst effect of drugs that prefer the continuous organic phase from hydrophobic polymer. The release rate from fibers containing surfactant after the drug's burst release was faster than the emulsion electrospun fibers. This may indicate that when initial water is added to the system in an emulsion, Rhodamine B prefers this water phase, and, therefore, more is encapsulated within the water phase leading to a slower diffusional drug release rate. It is also possible that the internal phase coalesced within these fibers to form a core of aqueous phase and drug, which would have a longer diffusional path than fibers with evenly distributed porosity. This is consistent with the hypothesis and studies conducted by Radisavljevic et al.[18] Further, Figure 5D illustrates a standard curve of Rhodamine B concentration illustrating the significant effect intermolecular interactions of the surfactant and Rhodamine B had on fluorescent values. Thus, the respective standard matching the fiber composition was used to calculate encapsulation efficiency and release for each of the groups.

Nile Red and Rhodamine B Release Comparison

Comparing all groups loaded with either Nile Red or Rhodamine B, fiber diameter and fiber fraction were not statistically different (Figure 6A and 6B). Controlling fiber diameter and fiber fraction while altering solution chemistry can be difficult because each component changes the behavior of the electrospinning jet during the electrospinning process. Controlling fiber diameter and fiber fraction also removes potentially confounding variables that can alter the interpretation of drug hydrophobicity and release rates because of the solvent. The amount of drug

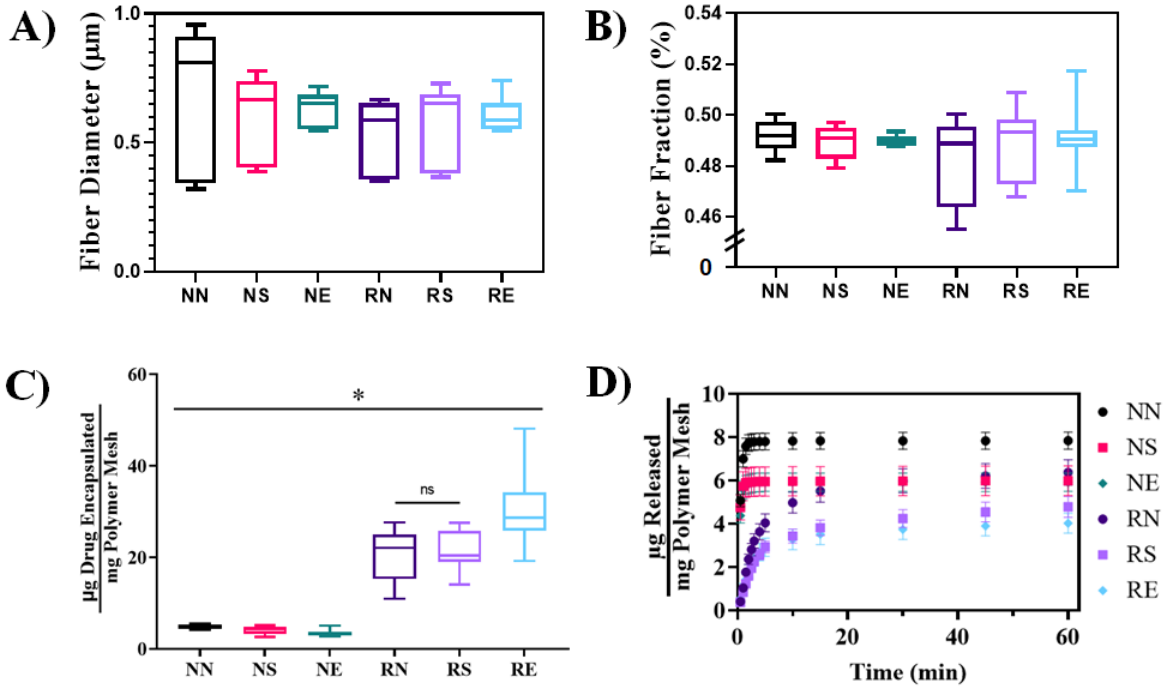

Figure 6: Comparison of fiber diameter (A), fiber volume fraction (B), mass encapsulated (C) and mass released (D) for all electrospun samples NN, NS, NE, RN, RS, and RE. Note that Nile Red was released in 100% ethanol and Rhodamine B was release in RO water. * $p \leq 0.05$; ** $p \leq 0.01$; *** $p \leq 0.001$; ****$p \leq 0.0001$

loaded into the scaffolds normalized for the weight of the sample was reduced in the Nile Red groups compared to the Rhodamine B groups highlighting the solubility preferences detailed previously (Figure **Error! Reference source not found.**6C). RE had the highest encapsulation of

drug for all samples as previously noted with Rhodamine B likely concentrated in the aqueous, internal phase based on relative hydrophilicity. Figure 6D illustrates relative release profiles for Nile Red in ethanol release media and Rhodamine B released in water. While the values are not directly comparable as these are two different release medias, the relative trends that were observed using these ideal solvents is of noting and further detailed in the best fit modeling. Future studies will assess release using a more physiologically relevant solvent such as PBS or simulated body fluid to directly compare release rates from hydrophobic and hydrophilic drugs.

Best Fit Drug Release Modeling

Least squares regression analysis was conducted to determine the best fit comparing four common models for release from cylinders including first-order, zero-order, Higuchi, and Ritger-Peppas. Figure 7 shows the results for each group and Table 1 and 2 display the release constant, K, and R^2 values, respectively. For release of both small molecules, first-order was the closest fit and

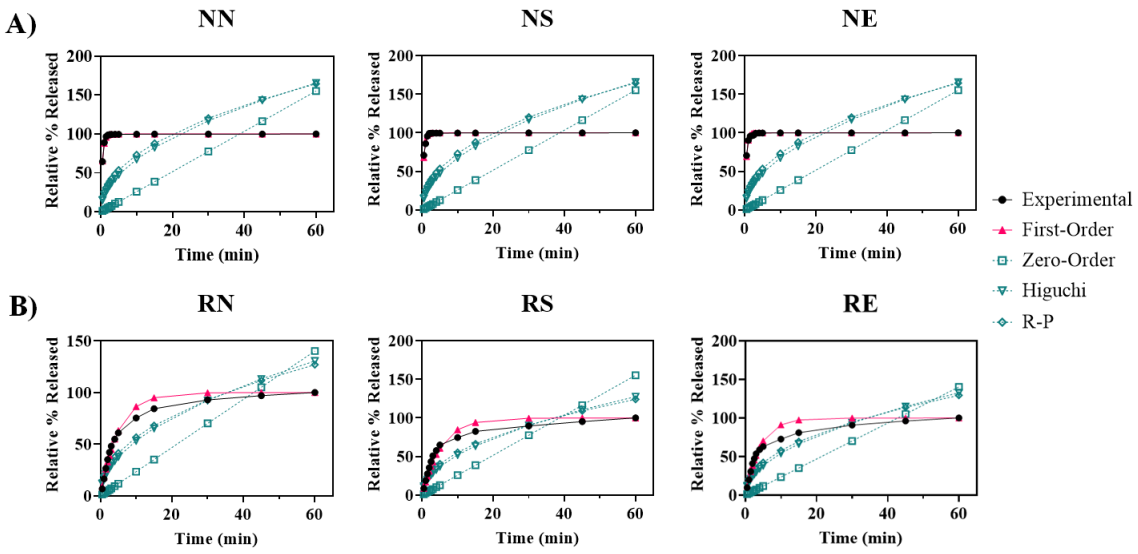

Figure 7: Linear regression analysis to determine the best fit model for Nile Red (A) and Rhodamine B (B) release. First-order, Zero-order, Higuchi, and Ritger-Peppas were used to determine release constant (K) values that best fit the experimental data for the one-hour release.

shows a dependence of the release on the concentration of encapsulated drug. Nile Red release

(Figure 7A) was closer to first-order release based on goodness of the fit compared to Rhodamine B (Figure 7B), which deviated from this profile at later time points within the hour release and suggest two-phases in the release. The larger K values for Nile Red release correlate to the faster burst release observed in all of these samples compared to the Rhodamine B. Further, with the Nile Red release data, the K values increase with addition of surfactant and the water phase in the emulsion groups release correlating with the increase in initial burst release rate at early time points in those groups compared to the control. Minimal differences in K values were observed in the groups with Rhodamine B release; however, this is only most acurate for the first 10 minutes of release after which the fit deviates from the experimental data. In the future, release over days will be conducted to assess changes to the release profile and the mechanism driving release over time.

Table 2. Release constant, K, values for the respective model best fit regression analysis

K Values						
	NN	**NS**	**NE**	**RN**	**RS**	**RE**
First-Order	2.13	2.29	2.37	0.20	0.19	0.24
Zero-Order	0.03	0.03	0.03	0.02	0.02	0.02
Higuchi	0.21	0.21	0.21	0.17	0.16	0.17
Ritger-Peppas	0.26	0.26	0.26	0.02	0.21	0.21

Table 3. R^2 values to assess fit of each model

R^2 Values						
	NN	**NS**	**NE**	**RN**	**RS**	**RE**
First-Order	0.99	0.97	0.98	0.97	0.95	0.92
Zero-Order	-62.88	-85.12	-91.75	-0.41	-0.67	-0.81
Higuchi	-32.17	-43.80	-47.21	0.68	0.60	0.54
Ritger-Peppas	-27.53	-37.55	-40.48	-2.63	0.71	0.67

Limitations

Using small molecule fluorophores to determine release was done in this study to initially determine relative release from each of the systems based on ability to use a spectrometer and

reduce the time and costs needed to optimize methods such as HPLC or ELISA, depending on the molecule chemistry. However, this approach results in the potential for photobleaching of the fluorophores during fabrication, encapsulation efficiency measurements, and release characterization studies. As such, future studies will characterize release as a function of molecule hydrophobicity using analytic methods that do not rely on fluorescence for quantification. Further, these initial release studies were conducted in release solvents in which the Nile Red and Rhodamine B were soluble. Future studies will focus on release in solutions analogous to physiological conditions including PBS or simulated body fluid at pH = 7.4 and 37°C.

Conclusions

Overall, the findings from this study illustrate the role of intermolecular interactions between surfactant and drug and phase solubility and preference, independent of fiber diameter, fiber volume fraction, on release rates of a model hydrophobic and hydrophilic drug. In the groups studied here, the drug-solvent solubility as dictated by drug hydrophobicity affected both drug loading and release. In the groups with Nile Red, emulsion fibers exhibited less encapsulation, but similar release rates compared to the surfactant control. However, with Rhodamine B, more drug was encapsulated based on solubility in the aqueous internal phase while the release rate was reduced indicating the ability to control release by tuning the internal phase and drug solubility. Current work is focused on changes to hydrophilic/lipophilic balance (HLB) of non-ionic surfactants based on changes to the chemistry to further probe the impact of intermolecular interaction of surfactant with drug molecules. Excitingly, this information will be used for future designs of fiber-based systems for drug release in tissue engineering applications.

Acknowledgements

The authors are grateful for Katie Donnelly's help preparing samples for drug release studies. This work was supported by startup funds from the University of Kansas (JR), NIH Biotechnology Training Grant (T32) Pharmaceutical Aspects of Drug Delivery (PJ), Howard Hughes Medical Institute James H. Gilliam Fellowship for Advanced Study (PJ and JR), and the KU Doctoral Student Research Fund (PJ).

Authorship CRediT

Pamela Johnson: Conceptualization (equal); Data curation (lead); Formal analysis (lead); Investigation (lead); Methodology (lead); Project administration (equal); Software (lead); Supervision (equal); Validation (lead); Visualization (lead); Writing-original draft (lead); Writing-review & editing (supporting)

Justin Lehtinen: Investigation (supporting); Methodology (supporting); Validation (supporting); Writing-review & editing (supporting)

Jennifer Robinson: Conceptualization (equal); Formal analysis (supporting); Funding acquisition (lead); Project administration (equal); Resources (lead). Supervision (equal); Validation (supporting); Visualization (supporting); Writing-original draft (supporting); Writing-review & editing (lead)

References

1. Cheng H, Yang X, Che X, Yang M, Zhai G. Biomedical application and controlled drug release of electrospun fibrous materials. *Mater Sci Eng C Mater Biol Appl.* 2018;90:750-763.
2. Weng L, Xie J. Smart electrospun nanofibers for controlled drug release: recent advances and new perspectives. *Current pharmaceutical design.* 2015;21(15):1944-1959.
3. Zeng J, Xu X, Chen X, et al. Biodegradable electrospun fibers for drug delivery. *Journal of Controlled Release.* 2003;92(3):227-231.
4. Chou SF, Carson D, Woodrow KA. Current strategies for sustaining drug release from electrospun nanofibers. *Journal of controlled release : official journal of the Controlled Release Society.* 2015;220(Pt B):584-591.
5. Hu X, Liu S, Zhou G, Huang Y, Xie Z, Jing X. Electrospinning of polymeric nanofibers for drug delivery applications. *Journal of controlled release : official journal of the Controlled Release Society.* 2014;185:12-21.
6. Lu Y, Huang J, Yu G, et al. Coaxial electrospun fibers: applications in drug delivery and tissue engineering. *Wiley Interdiscip Rev Nanomed Nanobiotechnol.* 2016;8(5):654-677.
7. Ball C, Chou SF, Jiang Y, Woodrow KA. Coaxially electrospun fiber-based microbicides facilitate broadly tunable release of maraviroc. *Mater Sci Eng C Mater Biol Appl.* 2016;63:117-124.
8. Sill TJ, von Recum HA. Electrospinning: applications in drug delivery and tissue engineering. *Biomaterials.* 2008;29(13):1989-2006.
9. Wang S-Q, He J-H, Xu L. Non-ionic surfactants for enhancing electrospinability and for the preparation of electrospun nanofibers. *Polym Int.* 2008;57(9):1079-1082.
10. Xu H, Li H, Chang J. Controlled drug release from a polymer matrix by patterned electrospun nanofibers with controllable hydrophobicity. *J Mater Chem B.* 2013;1(33):4182.
11. Chen SC, Huang XB, Cai XM, Lu J, Yuan J, Shen J. The influence of fiber diameter of electrospun poly(lactic acid) on drug delivery. *Fiber Polym.* 2012;13(9):1120-1125.
12. Gu X, Song X, Shao C, et al. Electrospinning of poly(butylene-carbonate): Effect of Solvents on the Properties of the Nanofibers Film. *Int J Electrochem Sc.* 2014;9:8045-8056.
13. Zhang X, Yin Q, Cui P, Liu Z, Gong J. Correlation of Solubilities of Hydrophilic Pharmaceuticals versus Dielectric Constants of Binary Solvents. *Ind Eng Chem Res.* 2012;51(19):6933-6938.
14. Zhang C, Feng F, Zhang H. Emulsion electrospinning: Fundamentals, food applications and prospects. *Trends in Food Science & Technology.* 2018;80:175-186.
15. Yazgan G, Popa AM, Rossi RM, et al. Tunable release of hydrophilic compounds from hydrophobic nanostructured fibers prepared by emulsion electrospinning. *Polymer.* 2015;66:268-276.
16. Johnson PM, Knewtson KE, Hodge JG, et al. Surfactant location and internal phase volume fraction dictate emulsion electrospun fiber morphology and modulate drug release and cell response. *Biomater Sci-Uk.* 2021.
17. Tipduangta P, Belton P, Fabian L, et al. Electrospun Polymer Blend Nanofibers for Tunable Drug Delivery: The Role of Transformative Phase Separation on Controlling the Release Rate. *Mol Pharm.* 2016;13(1):25-39.

18. Radisavljevic A, Stojanovic DB, Perisic S, et al. Cefazolin-loaded polycaprolactone fibers produced via different electrospinning methods: Characterization, drug release and antibacterial effect. *Eur J Pharm Sci.* 2018;124:26-36.
19. Greenspan P, Fowler SD. Spectrofluorometric studies of the lipid probe, nile red. *J Lipid Res.* 1985;26(7):781-789.
20. Küchler S, Abdel-Mottaleb M, Lamprecht A, Radowski MR, Haag R, Schäfer-Korting M. Influence of nanocarrier type and size on skin delivery of hydrophilic agents. *Int J Pharmaceut.* 2009;377(1-2):169-172.
21. Higuchi WI. Diffusional models useful in biopharmaceutics: drug release rate processes. *J Pharm Sci-Us.* 1967;56(3):315-324.
22. Ritger PL, Peppas NA. A simple equation for description of solute release I. Fickian and non-fickian release from non-swellable devices in the form of slabs, spheres, cylinders or discs. *Journal of controlled release.* 1987;5(1):23-36.
23. Santhanalakshmi J, Maya S. Solvent effects on reverse micellisation of Tween 80 and Span 80 in pure and mixed organic solvents. *Proc Intian Acad Sci.* 1997;109:22=38.
24. Liao Y, Zhang L, Gao Y, Zhu Z-T, Fong H. Preparation, characterization, and encapsulation/release studies of a composite nanofiber mat electrospun from an emulsion containing poly(lactic-co-glycolic acid). *Polymer.* 2008;49(24):5294-5299.
25. Hu J, Wei J, Liu W, Chen Y. Preparation and characterization of electrospun PLGA/gelatin nanofibers as a drug delivery system by emulsion electrospinning. *Journal of biomaterials science Polymer edition.* 2013;24(8):972-985.
26. Yan S, Xiaoqiang L, Shuiping L, Xiumei M, Ramakrishna S. Controlled release of dual drugs from emulsion electrospun nanofibrous mats. *Colloids Surf B Biointerfaces.* 2009;73(2):376-381.
27. Qi H, Hu P, Xu J, Wang A. Encapsulation of drug reservoirs in fibers by emulsion electrospinning: morphology characterization and preliminary release assessment. *Biomacromolecules.* 2006;7(8):2327-2330.
28. Burgess K, Li H, Abo-Zeid Y, Fatimah, Williams GR. The Effect of Molecular Properties on Active Ingredient Release from Electrospun Eudragit Fibers. *Pharmaceutics.* 2018;10(3).